J. Chem. Sci. Vol. 124, No. 1, January 2012, pp. 121–129.

Optimal control of the initiation of a pericyclic reaction in the electronic ground state[#]

TIMM BREDTMANN* and JÖRN MANZ*

Institut für Chemie und Biochemie, Freie Universität Berlin, Takustr. 3, 14195 Berlin, Germany
e-mail: bredt@chemie.fu-berlin.de; jmanz@chemie.fu-berlin.de

Abstract. Pericyclic reactions in the electronic ground state may be initiated by down-chirped pump-dump sub-pulses of an optimal laser pulse, in the ultraviolet (UV) frequency and sub-10 femtosecond (fs) time domain. This is demonstrated by means of a quantum dynamics model simulation of the Cope rearrangement of Semibullvalene. The laser pulse is designed by means of optimal control theory, with detailed analysis of the mechanism. The theoretical results support the recent experimental initiation of a pericyclic reaction. The present approach provides an important step towards monitoring asynchronous electronic fluxes during synchronous nuclear pericyclic reaction dynamics, with femto-to-attosecond time resolution, as motivated by the recent prediction of our group.

Keywords. Quantum dynamics; optimal control; pericyclic reaction; semibullvalene.

1. Introduction

Laser control of pericyclic reactions in their electronic ground states is a challenge in chemical reaction dynamics. Schwebel *et al.* in 1984[1] demonstrated an important mechanism, initiation by means of high overtone excitations of various mode selective vibrations, in the infrared (IR) frequency domain. This experimental success has served, in part, as motivation for our previous design of IR pump-dump laser pulse control of pericyclic reactions.[2–4] The approach relies, however, on a prerequisite which is difficult to satisfy, i.e., strong changes of the dipole along the reaction path. Recently, Iwakura, Yabushita and Kobayashi could demonstrate an alternative approach, i.e., initiation of a pericyclic reaction in the electronic ground state, by means of an ultrashort laser pulse in the ultraviolet (UV) frequency domain, within less than ten femtoseconds (fs).[5] Detailed analysis yields the mechanism, essentially intrapulse UV pump-dump control of the initiation. This stimulating experiment serves as the first, general motivation for the present work. Accordingly, we shall apply optimal control theory (OCT)[6–10] in order to design an ultrashort laser pulse which initiates a pericyclic reaction in the electronic ground state. The goal is to investigate whether the UV pump-dump type mechanism will indeed turn out as the most efficient way to start the reaction.

As specific system, we shall consider the degenerate 3,3-sigmatropic shift, or Cope rearrangement[11] of semibullvalene[2–4,12–34] (C_8H_8, SBV) in the electronic ground state, see figure 1. The reactant (R) has a chain of six carbon atoms C6=C7-C8-C2-C3=C4 (clockwise notation) which is transformed into another chain C2=C3-C4-C6-C7=C8 (same clockwise notation, keeping the labels of the carbon atoms) for the products (P); here R and P may be distinguished by isotopic labelling. Apparently, the carbon-carbon bond C8-C2 (clockwise notation) is broken during the pericyclic reaction, while the C4-C6 bond is formed. Moreover, the double bonds C3=C4 and C6=C7 are shifted to C2=C3 and C7=C8, respectively (double bond shifting, DBS). This pericyclic reaction is similar to the Cope rearrangement of 1,5-hexadiene, except that most of the large amplitude motions of 1,5-hexadiene are essentially frozen by the additional 'bridge' of carbon atoms C1-C5 in SBV. This constraint supports the simple one-dimensioal (1D) model for the Cope rearrangement of SBV which has been introduced in Reference 34, see also Reference 15.

Cope rearrangements of SBV and several derivatives have already served as touchstones for various properties that are related to pericyclic reactivity, from synthesis[12,16,21,22,29] via spectroscopy[13,15,20,24,27] and kinetics[13,14,19] to electronic structure[17,18,21–26,28–31,35] and the related thermochromicity,[3,21,22,24,29] *ab initio* molecular dynamics[32], the role of tunnelling[33], and the above-mentioned quantum dynamics simulations of IR pump-dump laser control.[2–4] In particular, quantum chemistry first principal calculations show that the Cope rearrangement of SBV in the electronic ground state

[#]Dedicated to Prof. N Sathyamurthy on his 60th birthday
*For correspondence

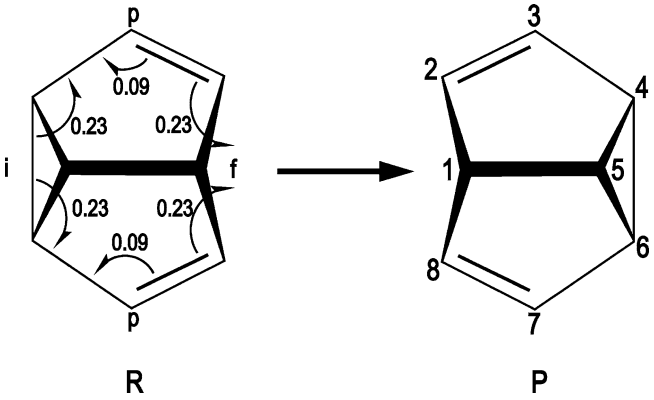

Figure 1. Cope rearrangement of semibullvalene, with pincer-motion-type directionality of electronic fluxes indicated by curved arrows in Lewis structures (adapted from Reference 34.) The numbers in the reactant structure R specify the amounts of pericyclic electrons which flow between neighbouring bonds. Symbols i and f indicate dominant initial and final fluxes of electrons, out of the bond to be broken and into the bond to be formed, respectively. Symbol p indicates perpetual weak electronic flux during double bond shifting. The labels for the carbon atoms (see product structure P) are the same for R and P.

proceeds in a symmetric double well potential energy surface (PES), with two equivalent minima representing R and P which are separated by a rather shallow barrier.[18,21,22,24,26,28–31,33] In contrast, in the first excited electronic state, SBV has a rather steep and deep symmetric single well PES with large energy gap to the potential barrier in the electronic ground state ($\Delta E \gg 2$ eV[18,20,24]).

Recently, we could determine the coupled electronic and nuclear fluxes during the Cope rearrangement of SBV.[34] The results of Reference 34 are quite surprising, in view of the traditional rules for the outcome and the associated net electron transfer during pericyclic reactions, which is symbolized by curved arrows in Lewis structures of the reactant[36], see e.g., the text books of organic[37–41], inorganic[42,43], and biochemistry.[44,45] The corresponding valence electrons which describe the changes of the Lewis structures, from R to P, are called 'pericyclic'. These electrons are complementary to other valence electrons (e.g., those representing CH bonds) or core electrons. Specifically, we were able to identify the directionality of the fluxes of 'pericyclic' electrons: It is well described by the pincer-motion-type (as opposed to clockwise or anticlockwise) pattern of the curved arrows, as illustrated in figure 1. Also, we discovered that the number of pericyclic electrons which is transferred per curved arrow, is typically between 0.09 and 0.23 i.e., much smaller than the traditional assumption of 1 or even 2. Furthermore, we detected significant opposite fluxes of other valence electrons. For the scenario of Reference 34, the time scale of the Cope rearrangement of SBV was determined to be less than 30 fs. Moreover, we could discover that various individual processes of the pericyclic reaction such as C8-C2 bond breaking, DBS from C3=C4 to C2-C3 as well as from C6=C7 to C7=C8, and C4-C6 bond formation, are associated with asynchronous electronic fluxes during synchronous nuclear motions. This is a significant extension of previous investigations which have centred attention on the simpler question of synchronicity or concertedness versus sequentiality, just for the nuclear motions during chemical reactions, while ignoring electronic motions, see e.g., References 35, 46 and 47. Some important results of Reference 34 are summarized in figure 1.

Certainly, it is a challenge to investigate the predictions of Reference 34 experimentally, using e.g., modern techniques of femto- to attosecond spectroscopy which allow to monitor the time evolutions of valence electrons[48–51], see also References 52–60 and the review 61. For this purpose, it will be necessary to initiate the Cope rearrangement of SBV in the electronic ground state. This request provides the second, specific motivation of this paper, that means we shall explore the efficiency of the intrapulse UV pump-dump mechanism of Iwakura, Yabushita and Kobayashi[5], for initiation of the specific pericyclic reaction, Cope rearrangement of SBV in the electronic ground state. For this purpose, we shall adapt the same 1D model for the nuclear wavepacket dynamics which has been employed in Reference 34, with extensions based on Reference 2. The results for this idealized scenario should serve as a reference for accurate quantum simulations of more demanding realistic models.

This paper presents the model and techniques, the results and discussion followed by conclusions in sections 2, 3 and 4, respectively.

2. Model and techniques

The subsequent quantum simulations of the nuclear wave packet dynamics representing the laser driven pericyclic reaction of SBV employ the simple model of Reference 34. It is illustrated in figure 2. The model is motivated by the constrained mobility of SBV, as outlined in section 1, and also by the fact that for the scenario of Reference 34, the transformation from R to P takes less than 30 fs. This suggests that the reaction should be induced by exciting a distinguished 'reactive' nuclear degree of freedom (dof), called ξ, such

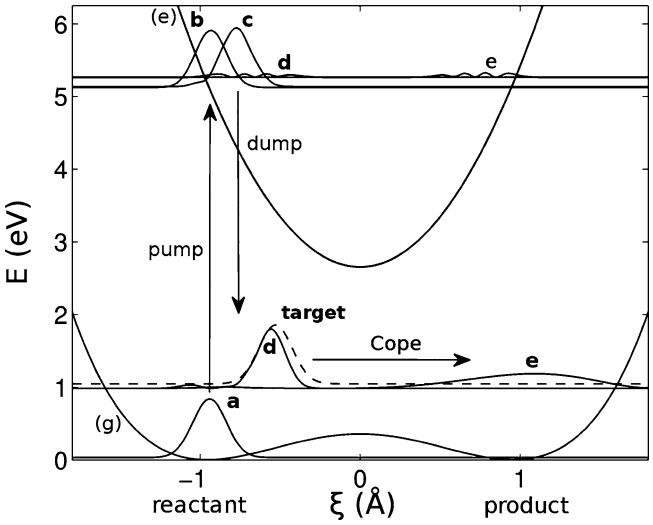

Figure 2. Optimal control of the initiation of the Cope rearrangement of semibullvalene (SBV) in the electronic ground state. The time evolution of the laser driven wavepacket dynamics from the reactant (R) along the nuclear coordinate ξ to the product (P), is illustrated by the series of snapshots 'a,b,c,d,e' of the nuclear densities, at times $t =$ 0.0 fs, 3.1 fs, 7.1 fs, 10.0 fs (the end of the laser pulse) and $t = 33.5$ fs, respectively. They are embedded in the potential energy surfaces of SBV in the electronic ground and excited states, $V_g(\xi)$ and $V_e(\xi)$, adapted from References 34 and 2, respectively. The asymptotic base lines of the densities correspond to their mean energies. Also shown is the density of the target state, eqn. (5), adapted from Reference 34 which runs from R to P, with total energy E well above the barrier of $V_g(\xi)$ (dashed line). Snapshot 'a' shows the density of the initial ground state $\Psi_{g,v=0}(\xi)$ of R, with energy $E_{g,v=0}$. Snapshots 'b,c,d' illustrate the evolution in the electronic excited state, $V_e(\xi)$, mediated by the pump and dump sub-pulses of the optimal control pulse, which are indicated by the vertical arrows. Snapshot 'd' embedded in $V_g(\xi)$ shows the density of the wavepacket at the end of the laser pulse, $t = \tau$, close to the 'target' state. Subsequently, it evolves to snapshot 'e' representing the product P in the electronic ground state. A small fraction of the total density is left in the excited electronic state, and runs simultaneously from snapshot 'd' to 'e' embedded in $V_e(\xi)$.

that motion along ξ is much faster than any competing process such as intramolecular vibrational redistribution (IVR) of the available energy from ξ to the other $3\times16-6-1 = 41$ 'passive' vibrational dofs. The single dof ξ that we consider leads straight from the minimum of the symmetric double well PES representing R to the other one representing P. It accounts for synchronous motions of all the nuclei during the pericyclic reaction. As dominant large amplitude motion, it describes the difference of the lengths of the two carbon-carbon bonds C8-C2 and C4-C6 (clockwise notation, cf. figure 1) which are broken and formed, respectively, during the Cope rearrangement, see also Reference 15, confirmed by Reference 32. Accordingly, the values ξ_R and ξ_P of ξ at the potential minima representing R and P have the same absolute values, but opposite signs, see figure 2. The associated reduced mass is $\mu = (M_C + M_H)/4$.[15] The 1D curve of the PES $V_g(\xi)$ of SBV in the electronic ground (g) state which is shown in figure 2 is adapted from Reference 34. It was evaluated by means of quantum chemical first principles calculations based on Kohn-Sham density functional theory. The calculations are performed with the MOLPRO[62] program package, using the B3LYP functional[63,64] together with the cc-pVTZ[65] basis sets. The reliability of this method concerning structures and energies along the coordinate ξ is ensured by comparison to high-level *ab initio* methods (CASPT2/cc-pVTZ and MRCI/cc-pVTZ, CCSD(T)/cc-pVTZ, respectively). In addition, the PES of SBV in the excited (e) state is modelled as harmonic potential with empirical parameters, as derived in Reference 2.

The initial (t = 0) state of the system representing R is the vibrational ground state ($v = 0$) which is localized in the potential well of the electronic ground state (g) representing R, $\Psi_g(t = 0) = \Psi_{g,v=0}$, without any component in the excited electronic state (e), $\Psi_e(t = 0) = 0$. The density $\rho_{g,v=0}(\xi) = |\Psi_{g,v=0}(\xi)|^2$ is shown as wavepacket labelled 'a' in figure 2. The time evolution of the laser driven wavepackets, $\Psi_g(t > 0)$ and $\Psi_e(t > 0)$, is obtained as solution of the time-dependent Schrödinger equation (TDSE), in semiclassical dipole approximation,

$$i\hbar\frac{\partial}{\partial t}\begin{pmatrix}\Psi_e(t)\\ \Psi_g(t)\end{pmatrix} = \left[\begin{pmatrix}T+V_e & 0\\ 0 & T+V_g\end{pmatrix} - \mathcal{E}(t)\begin{pmatrix}d_{ee} & d_{eg}\\ d_{ge} & d_{gg}\end{pmatrix}\right]\begin{pmatrix}\Psi_e(t)\\ \Psi_g(t)\end{pmatrix}. \quad (1)$$

The rather simple form of the TDSE (1) applies to the scenario of a pre-oriented, non-rotating molecule interacting with a linearly polarized laser pulse. Pre-orientation may be achieved e.g., by the methods of References 66–69. The laser pulse with electric field component $\mathcal{E}(t)$ should then be polarized parallel to the transition dipole between the ground (g) and excited (e) electronic state. The relevant component is modelled as $d_{eg} = d_{ge} = 0.3934\,ea_0 = 1$ debye in Condon approximation. Furthermore, we neglect the dipole functions, $d_{gg} = d_{ee} = 0$. The experiment of Reference 5 suggests a rather short duration τ of the laser pulse; we set $\tau = 10$ fs. Molecular rotations are negligible, indeed, on this time scale. As a consequence, the model describes nuclear motions exclusively along ξ, with kinetic energy operator $T = -\hbar^2/(2\mu) \times \partial^2/\partial\xi^2$. Kinetic

couplings are also neglected, in Born-Oppenheimer approximation.

The wavefunctions $\Psi_g(\xi, t)$ and $\Psi_e(\xi, t)$ allow to calculate all the properties which are important for the subsequent analysis, including the densities

$$\begin{aligned} \rho_g(t) &= |\Psi_g(\xi, t)|^2 \\ \rho_e(t) &= |\Psi_e(\xi, t)|^2, \end{aligned} \tag{2}$$

the populations

$$\begin{aligned} P_g(t) &= \langle \Psi_g(t) | \Psi_g(t) \rangle \\ P_e(t) &= \langle \Psi_e(t) | \Psi_e(t) \rangle \end{aligned} \tag{3}$$

where $\langle \ldots | \ldots \rangle$ denotes integration over the nuclear coordinate ξ, and the energies

$$\begin{aligned} E_g(t) &= \langle \Psi_g(t) | T + V_g | \Psi_g(t) \rangle / P_g(t), \\ E_e(t) &= \langle \Psi_e(t) | T + V_e | \Psi_e(t) \rangle / P_e(t). \end{aligned} \tag{4}$$

The double-motivated, specific goal of the present investigation is to design a laser pulse $\mathcal{E}(t)$ which initiates the Cope rearrangement of SBV in the electronic ground state, starting from the ground state $\Psi_g(\xi, t = 0) = \Psi_{g,v=0}(\xi)$ and yielding essentially the same wavepacket dynamics as in Reference 34. For this purpose, we request that at the end ($t = \tau$) of the laser pulse, the laser driven wavepacket $\Psi_g(\xi, t = \tau)$ should agree with the reactant wavefunction of Reference 34, soon after the start of the Cope rearrangement – this wave function will be called the 'target wave function $\Psi_{g,\text{target}}(\xi)$'. For convenience, we employ

$$\Psi_{g,\text{target}}(\xi) \approx \Psi_{g,v=0}(\xi - \Delta\xi) \times e^{ik\xi}. \tag{5}$$

The density of $\Psi_{g,\text{target}}(\xi)$ is illustrated in figure 2 by the dashed line. Apparently, the first factor in eqn. (5) describes the shift of the initial wavefunction from its centre at ξ_R to $\xi_{\text{target}} = \xi_R + \Delta\xi$, soon after the start of the reaction, but before the onset of wavepacket dispersion. For the present application, we use $\Delta\xi = 0.41$ Å. The second factor $e^{ik\xi}$ describes nuclear motions directed from R to P, with momentum $\hbar k$. The corresponding kinetic and total energies are $E_{\text{kin}} = \hbar k^2/(2\mu)$ and

$$E_g = E_{\text{kin}} + V_g(\xi_{\text{target}}), \tag{6}$$

respectively. The target value $E_g = 1.04$ eV is adapted from Reference 34, so that perfect generation of the target wavepacket, eqn. (5), launches the same wavepacket dynamics of SBV, from R to P, as in Reference 34.

The design of the laser pulse $\mathcal{E}(t)$ which drives the initial wavefunction $\Psi_g(\xi, t = 0) = \Psi_{g,v=0}(\xi)$ to the target wavefunction, eqn. (5), is achieved by means of OCT.[6–10] It maximizes the cost functional, that means the absolute value of the overlap, $|\langle \Psi_{g,\text{target}} | \Psi_g(t = \tau) \rangle|$ at the end ($t = \tau$) of the laser pulse, subject to the ubiquitious 'penalty' for all-too-strong electric field strengths.[6–10] In practice, we employ the version of OCT as implemented in the Multi Configuration Time Dependent Hartree (MCTDH) package for propagation of (laser driven) nuclear wavepackets, as documented in References 70–72. The perfect laser pulse should yield the ideal value $|\langle \Psi_{g,\text{target}} | \Psi_g(t = \tau) \rangle| = 1$ – this would guarantee that the subsequent ($t > \tau$) free evolution of $\Psi_g(\xi, t)$ is the same as in Reference 34.

3. Results and discussion

The optimal laser pulse $\mathcal{E}(t)$ and the resulting population dynamics, $P_g(t)$, $P_e(t)$, are documented in the middle and bottom panels of figure 3, respectively. The interpretation is obvious: the optimal laser pulse consists of two sub-pulses which 'pump' and 'dump' populations, first from the electronic ground to the excited state, and then back to the ground state. Subsequently, we shall analyse these sub-pulses in order to discover their cooperative mechanisms, which allow them to reach the present goal of laser control, that is initiation of the Cope rearrangement of the model SBV, from R to P, in the electronic ground state, equivalent to the reaction dynamics in Reference 34, *cum grano salis*. We shall also discuss some remaining drawbacks.

The first and second sub-pulse are well separated from each other — apparently, they have different tasks which need to be carried out at special times with selective time delay t_d. Specifically, they are centered at $t_{\text{pump}} = 2.4$ fs and at $t_{\text{dump}} = 7.7$ fs , respectively, thus $t_d = 5.3$ fs, and they last from approximately $t = 1.7$ fs till $t = 3.1$ fs and from $t = 7.1$ fs till $t = 8.3$ fs, respectively, i.e., they have similar durations of 1.4 fs and 1.2 fs, respectively. They consist of a little less than four and about three half-cycles, respectively, implying an overall down chirp, that means larger frequency of the pump sub-pulse than for the dump sub-pulse (see figure 2, top panel). The corresponding photon energies are resonant or near-resonant to the energy gaps of the PES,

$$\begin{aligned} \hbar\omega_{\text{pump}} &\approx V_e(\xi_{\text{pump}}) - V_g(\xi_{\text{pump}}) \approx 5.1\,\text{eV} \\ \hbar\omega_{\text{dump}} &\approx V_e(\xi_{\text{dump}}) - V_g(\xi_{\text{dump}}) \approx 4.1\,\text{eV} \end{aligned} \tag{7}$$

at the positions $\xi_{\text{pump}} = \xi_R = -0.94$ Å and $\xi_{\text{dump}} = -0.74$ Å. This supports resonant population transfer by vertical Franck-Condon (FC) type pump and dump transitions at ξ_{pump} and ξ_{dump}, respectively. These positions and the transitions are indicated by the vertical arrows in figure 2. Note that the resonant position ξ_{dump}

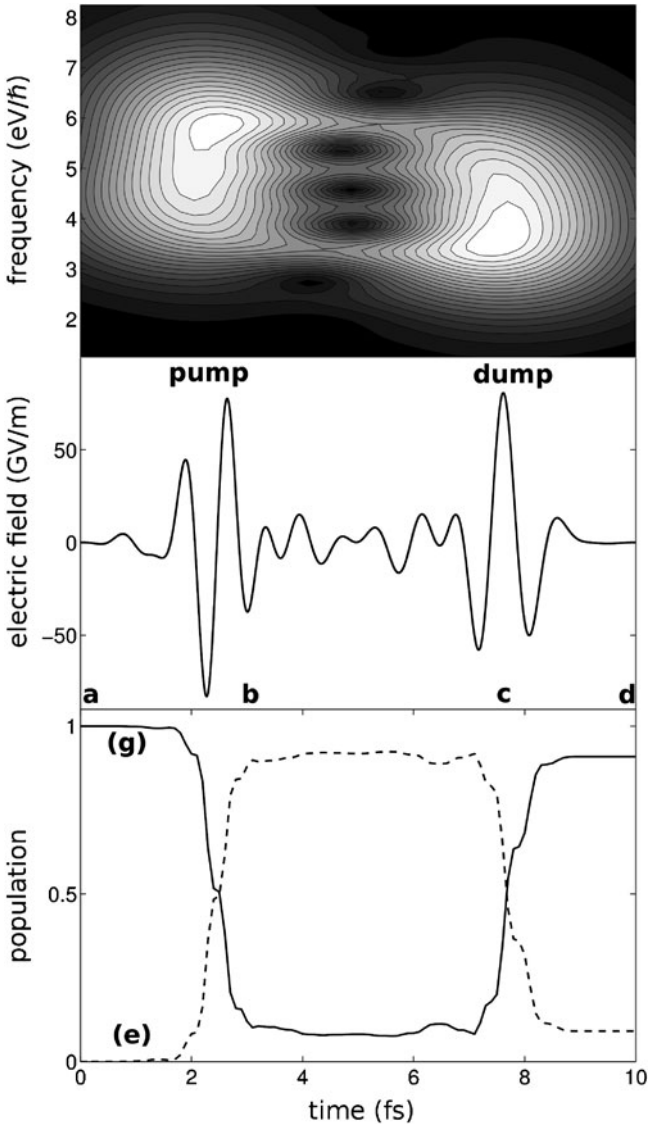

Figure 3. Optimal laser pulse $\mathcal{E}(t)$ for control of the initiation of the Cope rearrangement of semibullvalene SBV (middle panel), and the resulting population dynamics $P_g(t)$ and $P_e(t)$ in the electronic ground (g) and excited (e) states, respectively (bottom panel). The events labelled 'a,b,c,d' correspond to the snapshots of the laser-driven wavepacket dynamics shown in figure 2. Obviously, the optimal control pulse consists of two sub-pulses which induce the 'pump' and 'dump' transitions, as indicated in figure 2. The laser pulse and the resulting population dynamics are switched off at $\tau = 10$ fs. The top pannel shows the time-frequency profile of the optimal pulse, obtained by a Gabor transform using a Gaussian time-window (see e.g., References 73,74).

of the dump sub-pulse is located slightly before the centre ξ_{target} of the target wavepacket $\Psi_{g,\text{target}}(\xi)$, cf. figure 2. This allows to generate $\Psi_g(\xi, t)$ with proper kinetic and total energies (see below) at $t = t_{\text{dump}} = 7.7$ fs, readily before the final time $\tau = 10$ fs when the laser pulse is switched off, after driving the wavepacket $\Psi_g(\xi, t = \tau)$ as close to the target $\Psi_{g,\text{target}}(\xi)$ as possible. The criterion for the decisive value, $\xi_{\text{dump}} = -0.74$ Å, will be quantified below.

The half cycles of the pump and dump sub-pulses have rather strong field amplitudes, with maximum absolute value $\mathcal{E}_{\max} \approx 80\,\text{GV/m}$ corresponding to maximum transient intensity, $I_{\max} = c\epsilon_0\mathcal{E}^2_{\max} = 1.7 \times 10^{15}\,\text{W/cm}^2$. The value of the integral $\int \mathcal{E}(t)dt = 0.23\,\frac{\text{GV}}{\text{m}}\text{fs}$ is much smaller than $\mathcal{E}_{\max}\tau = 800\,\frac{\text{GV}}{\text{m}}\text{fs}$, in accord with References 75,76. Close inspection of figure 3 shows that most of the populations are transferred at times close to the maxima or minima of the half cycles of the pump and dump sub-pulses. In contrast, rather small amounts of population are transferred whenever the electric field is close to zero, switching sign. As a consequence, the population transfers proceed in a stepwise manner, as documented in figure 3.

The laser driven wavepacket dynamics is illustrated in figure 2 by the snapshots of the corresponding densities, eqn. (2), labelled 'a,b,c,d,e', which are embedded in the respective PESs of the electronic ground and excited states. The choice of these snapshots has been made in order to explain the mechanism of the optimal laser pulse. Apparently, its pump sub-pulse transfers the original wavefunction $\Psi_{g,v=0}(\xi)$ (snapshot 'a') to $\Psi_e(\xi, t)$ in the excited electronic state (snapshot 'b'). The resonance condition, eqn. (7), of the FC-type vertical transition at $\xi = \xi_{\text{pump}} = \xi_R$ implies that $\Psi_e(\xi, t)$ is generated with energy

$$E_e(t) \approx E_e = V_g(\xi_R) + \hbar\omega_{\text{pump}} = V_e(\xi_R), \qquad (8)$$

which remains approximately constant during the time window between the pump and dump sub-pulses. The strong force of the steep repulsive wall of $V_e(\xi)$ close to $\xi = \xi_{\text{pump}} = \xi_R$ drives the wavepacket $\Psi_e(\xi, t)$ from R toward P. This is illustrated by the shift of the snapshot 'b' to 'c'. At the same time, the wavefunction $\Psi_e(\xi, t)$ gains momentum directed from R to P, and corresponding kinetic energy. Approximate conservation of energy during the time window between the pump and dump laser pulses implies that the kinetic energy of $\Psi_e(\xi, t)$ is approximately equal to

$$E_e(t) - V_e(\xi) \approx V_e(\xi_R) - V_e(\xi), \qquad (9)$$

where ξ denotes the centre (mean value) of $\Psi_e(\xi, t)$.

Next, the second sub-pulse dumps $\Psi_e(\xi, t)$ back to $\Psi_g(\xi, t)$ in the ground state, again in a vertical FC-type manner, located at ξ_{dump} and applied at t_{dump}. The time delay $t_d = t_{\text{dump}} - t_{\text{pump}}$ between the pump and dump sub-pulses corresponds to the time that $\Psi_e(\xi, t)$ needs to run from $\xi_{\text{pump}} = \xi_R$ to ξ_{dump}. Also, the value of ξ_{dump}

determines the optimal transition frequency or photon energy $\hbar\omega_{\mathrm{dump}}$, according to eqn. (7). Finally, the time from t_{dump} to τ is essentially the time $\Psi_{\mathrm{g}}(\xi, t)$ needs to run from ξ_{dump} till ξ_{target}. The resulting wavepacket $\Psi_{\mathrm{g}}(\xi, t = \tau)$ is illustrated by the snapshot labelled 'd' embedded in $V_{\mathrm{g}}(\xi)$.

The preceding analysis thus leaves us with the task to determine the parameter ξ_{dump} of the dump sub-pulse, for comprehensive understanding of the entire optimal laser pulse. The solution is as follows: By its FC nature, the dump sub-pulse is not only vertical, conserving the nuclear position at ξ_{dump}, but it also conserves nuclear momentum and, therefore, kinetic energy, thus

$$\begin{aligned} V_{\mathrm{e}}(\xi_{\mathrm{R}}) - V_{\mathrm{e}}(\xi_{\mathrm{dump}}) &= E_{\mathrm{g}}(t_{\mathrm{dump}}) - V_{\mathrm{g}}(\xi_{\mathrm{dump}}) \\ &\approx E_{\mathrm{g}} - V_{\mathrm{g}}(\xi_{\mathrm{dump}}). \end{aligned} \tag{10}$$

For the given PES $V_{\mathrm{g}}(\xi)$ and $V_{\mathrm{e}}(\xi)$ of the model SBV, for the given initial and target wavefunctions, and for the given duration τ of the optimal laser pulse, the equation (10), combined with the previous ones (6) – (9), imposes the total energy (6) of the target wavefunction (5) as decisive contraint, which determines all the frequencies and the timing of the two pump and dump sub-pulses of the optimal laser pulse. The second equation (10) is based on approximate conservation of the total energy, during the time window from the dump sub-pulse till the end ($t = \tau$) of the optimal laser pulse.

Comparison of the laser driven wavefunction $\Psi_{\mathrm{g}}(\xi, \tau)$ and the target wave function $\Psi_{\mathrm{g,target}}(\xi)$ shows good but not perfect agreement; for the energies, locations, and shapes, see figure 2. As a consequence, the subsequent free evolution of $\Psi_{\mathrm{g}}(\xi, t)$ for $t > \tau$ is also similar to the free evolution of the target wavefunction, which has been adapted from, and which is documented in Reference 34. Snapshot 'e' shows the density of $\Psi_{\mathrm{g}}(t = t_{\mathrm{P}})$ on arrival at the product configuration P, i.e., when it is centred at ξ_{P}. As expected, it agrees almost perfectly with the corresponding snapshot of the product wavefunction which is shown in figure 1 of Reference 34.

As a summary, the optimal laser pulse $\mathcal{E}(t)$ shown in figure 3 fulfils its task, i.e., it initiates the Cope rearrangement of the model SBV in the electronic ground state so that the resulting wavepacket dynamics from R to P is similar to that of Reference 34. Close analysis reveals, however, that $\mathcal{E}(t)$ is not perfect. First of all, its pump sub-pulse does not achieve perfect population transfer from the electronic ground to the excited state. Figure 3 shows that the population which remains in $V_{\mathrm{g}}(\xi)$ is about $P_{\mathrm{g}}(t) \approx 0.08$, from $t \approx 3$ fs till 7 fs. As a consequence, $\Psi_{\mathrm{g}}(\xi, t)$ keeps a small partial wave which remains trapped in the reactant well of $V_{\mathrm{g}}(\xi)$. This partial wave is not an eigenstate, hence it exhibits non-stationary dynamics. This is visible in the time evolution of the small lobes of the densities $\rho_{\mathrm{g}}(\xi, t)$ labelled 'd' and 'e', close to $\xi = \xi_{\mathrm{R}}$. Similar effects of a pump pulse, called 'hole carving' in the ground state wavepacket, have been discovered first by Kosloff and coworkers.[77,78] Likewise, the dump sub-pulse does not achieve perfect population transfer from the excited electronic state back to the ground state. This is documented by the rather small but clearly non-vanishing densities $\rho_{\mathrm{e}}(\xi, t)$ labelled 'd' and 'e', embedded in $V_{\mathrm{e}}(\xi)$, see figure 2. These deficiencies could possibly be eliminated by even larger field strength, but in practice, this is prohibitive due to competing effects such as excitations of higher electronic states, or ionization.

4. Conclusions

The present model investigation confirms the general experimental result of Reference 5, which has served as first, general motivation, i.e., pericyclic reactions in the electronic ground state may be induced by laser pulses in the visible to UV frequency and sub-10-fs time domains. OCT yields a down-chirped intra-pulse pump-dump mechanism as the most efficient approach towards this goal. The two pump and dump sub-pulses induce resonant FC-type transitions, from the ground to the electronic excited state, and back, with optimal time delay. In contrast, Reference 5 employs non-resonant sub-pulses. The present results suggest that the efficiency of the experiment may be enhanced by means of properly chirped resonant ones. In any case, the sub-pulses of Reference 5 and the present one are few (one to two) cycle pulses, with corresponding broad spectral ranges (approximately 1 eV). This supports the rather flexible generation of suitable time-dependent nuclear wavepackets, which may consist of several vibrational eigenstates, first in the excited electronic state and subsequently in the electronic ground state, as documented in figure 2.

The intrapulse pump–dump mechanism of the present optimal laser pulse is somewhat analogous to the original pump-dump mechanism of Tannor and Rice[6,9,10], but there are important differences: Their motivation has been laser control of photodissociations towards competing product channels; they were able to achieve this goal by means of OCT in the weak field limit, at the expense of rather low product yields.[6] In contrast, we aim at a new task of laser control (compare e.g., with References 79, 80) that is initiation of a unimolecular reaction, exclusively in the electronic ground state, and with perfect product yield. For this

purpose, we have to employ OCT in the strong field limit.[7,8] The analysis of the mechanism in section 3 suggests to design analytical laser pulses e.g., with Gaussian envelopes and similar frequencies, durations and time delay, lending themselves more easily to experimental applications than those obtained by means of OCT. In any case, the present laser pulse is complementary to previous down-chirped intra-pulse pump-dump laser pulses which serve different purposes, e.g., to induce large amplitude vibrations in the electronic ground state[81,82], or control of branching ratios and photodesorption yields.[83]

The present results are encouraging also concerning the second, specific motivation, that means to pave the way towards experimental monitoring the electronic fluxes during the Cope rearrangement of SBV in the electronic ground state, as predicted in Reference 34, cf. figure 1. At the same time, it calls for several extensions, e.g., the present empirical potential $V_e(\xi)$ of the electronic excited state should be replaced by quantum chemical *ab initio* calculations, and the simple 1D model should be replaced by a multi-dimensional one. For example, the forces of the PES in the electronic excited state V_e, and subsequently also in the ground state V_g, may possibly (but not neccessarily, depending on the system) drive the wavepackets $\Psi_e(t)$ and subsequently also $\Psi_g(t)$ away from the ideal 'shortcut' along ξ – this may cause excitations of several vibrational modes in the product P, as observed in Reference 5; for an early, illuminating discussion of the relations of potential energy surfaces and molecular reaction dynamics, see e.g., Reference 84. In order to suppress these competing channels, one may employ the tools of Reference 85, compare with Reference 86.

Another challenge is perfect suppression of any partial wave $\Psi_e(t)$ which 'survives' in the electronic excited state, after the optimal laser pulse. This task is motivated by the work of the group of Takatsuka *et al.*[87–89], which implies that the interplay of the ground state wave function $\Psi_g(t)$ with even just a small component of $\Psi_e(t)$ might have a rather strong effect on the results for the net electronic fluxes from R to P in the electronic ground state. This task may be supported by model systems with shallower PES V_e in the electronic excited case, supporting perfect generation and subsequent annihilation of slower wavepackets $\Psi_e(t)$ by means of longer and less intense pump and dump sub-pulses. Alternatively, following a suggestion of Prof. W Jakubetz (Universität Wien), one might employ another laser pulse which eliminates any remaining components of $\Psi_e(t)$, by means of state-(e)-selective photoionization.

Work along these lines is in progress.

Acknowledgements

We would like to thank Professor W Jakubetz (Universität Wien) for stimulating discusssions of the present OCT results, and to Professor B Paulus (Freie Universität Berlin) for helpful advice on the underlying applications of the quantum chemistry, and to Dr. M Schröder (Universität Heidelberg) for advice on the OCT implementation in the MCTDH program package. Generous financial support by the Deutsche Forschungsgemeinschaft DFG, project Ma515/25-1, and by the Fonds der Chemischen Industrie FCI are also gratefully acknowledged.

References

1. Schwebel A, Brestel M and Yogev A 1984 *Chem. Phys. Lett*. **107** 579
2. Dohle M, Manz J and Paramonov G K 1995 *Ber. Bunsenges. Phys. Chem*. **99** 478
3. Dohle M, Manz J, Paramonov G K and Quast H 1995 *Chem. Phys*. **197** 91
4. Korolkov M V, Manz J and Paramonov G K 1996 *J. Chem. Phys*. **105** 10874
5. Iwakura I, Yabushita A and Kobayashi T 2010 *Chem. Lett*. **39** 374
6. Tannor D J and Rice S A 1985 *J. Chem. Phys*. **83** 5013
7. Peirce A P, Dahleh M A and Rabitz H 1988 *Phys. Rev. A* **37** 4950
8. Jakubetz W, Manz J and Schreier H-J 1990 *Chem. Phys. Lett*. **165** 100
9. Rice S A and Zhao M 2000 *Optical Control of Molecular Dynamics* (John Wiley & Sons, New York)
10. Shapiro M and Brumer P 2003 *Principles of the quantum control of molecular processes* (Wiley, New Jersey)
11. Cope A C and Hardy E M 1940 *J. Am. Chem. Soc*. **62** 441
12. Zimmerman H E and Grunewald G L 1966 *J. Am. Chem. Soc*. **88** 183
13. Cheng A K, Anet F A L, Mioduski J and Meinwald J 1974 *J. Am. Chem. Soc*. **96** 2887
14. Martin H-D and Urbanek T 1985 *J. Am. Chem. Soc*. **107** 5532
15. Bergmann K, Görtler S, Manz J and Quast H 1993 *J. Am. Chem. Soc*. **115** 1490
16. Quast H, Herkert T, Witzel A, Peters E M, Peters K and von Schnering H G 1994 *Chem. Ber*. **127** 921
17. Williams R V and Kurtz H A 1994 *J. Chem. Soc. Perkin Trans. 2* **2** 147
18. Jiao H, Nagelkerke R, Kurtz H A, Williams R V, Borden W T and von Ragué Schleyer P 1997 *J. Am. Chem. Soc*. **119** 5921
19. Jackman L M, Fernandes E, Heubes M and Quast H 1998 *Eur. J. Org. Chem*. 2209
20. Quast H and Seefelder M 1999 *Angew. Chem. Int. Ed*. **38** 1064
21. Williams R V 2001 *Eur. J. Org. Chem*. 227
22. Williams R V 2001 *Chem. Rev*. **101** 1185
23. Staroverov V N and Davidson E R 2001 *J. Mol. Struct*. **573** 81

24. Goren A C, Hrovat D A, Seefelder M, Quast H and Borden W T 2002 *J. Am. Chem. Soc*. **124** 3469
25. Garavelli M, Bernardi F, Cembran A, Castaño O, Frutos L M, Merchán M and Olivucci M 2002 *J. Am. Chem. Soc*. **124** 13770
26. Brown E C, Henze D K, and Borden W T 2002 *J. Am. Chem. Soc*. **124** 14977
27. Seefelder M, Heubes M, Quast H, Edwards W D, Armantrout J R, Williams R V, Cramer C J, Goren A C, Hrovat D A, and Borden W T 2005 *J. Org. Chem*. **70** 3437
28. Shaik S S and Hiberty P C 2008 *A chemist's guide to valence bond theory* (Wiley, Hoboken)
29. Williams R V 2009 *Strained hydrocarbons* (Wiley, Weinheim) pp. 399–424
30. Brown E C, Bader R F W and Werstiuk N H 2009 *J. Phys. Chem. A* **113** 5254
31. Greve D R 2010 *J. Phys. Org. Chem*. **24** 222
32. Rozgonyi T, Bartók-Pártay A and Stirling A 2010 *J. Phys. Chem. A* **114** 1207
33. Zhang X, Hrovat D A and Borden W T 2010 *Org. Lett*. **12** 2798
34. Andrae D, Barth I, Bredtmann T, Hege H-C, Manz J, Marquardt F and Paulus B 2011 *J. Phys. Chem. B* **115** 5476
35. Dewar M J S 1984 *J. Am. Chem. Soc*. **106** 209
36. Desimoni G, Tacconi G, Barco A and Pollini G P 2007 *Natural products synthesis through pericyclic reactions* (American Chemical Society, Washington, DC)
37. Berson J A 1980 *Rearrangements in ground and excited states, Vol. 1* (Academic Press, New York) p. 311
38. Lowry T H and Richardson K S 1987 *Mechanism and theory in organic Chemistry* (Harper and Row, New York)
39. Anslyn E V and Dougherty D A 2006 *Modern physical organic chemistry* (University Science Books, Sausalito)
40. Smith M B and March J 2007 *Advanced organic chemistry reactions, mechanisms, and structure* (Wiley, Hoboken)
41. Vollhardt K P C and Schore N E 2007 *Organic chemistry – structure and function* (Freeman, New York)
42. Wilkins R G 1991 *Kinetics and mechanism of reactions of transition metal complexes* (Verlag Chemie, Weinheim)
43. Jordan R B 2007 *Reaction mechanisms of inorganic and organometallic systems* (Oxford University Press, Oxford)
44. Mathews C K, van Holde K E and Ahern K G 1999 *Biochemistry* (Prentice Hall, Upper Saddle River)
45. Nelson D L and Cox M M 2009 *Lehninger principles of biochemistry* (Freeman, New York)
46. Borden W T, Loncharich R J, and Houk K N 1988 *Ann. Rev. Phys. Chem*. **39** 213
47. Xu L, Doubleday C E and Houk K N 2010 *J. Am. Chem. Soc*. **132** 3029
48. McFarland B K, Farrell J P, Bucksbaum P H and Gühr M 2008 *Science* **322** 1232
49. Bisgaard C Z, Clarkin O J, Wu G, Lee A M D, Geßner O, Hayden C C and Stolow A 2009 *Science* **323** 1464
50. Wörner H J, Bertrand J B, Kartashov D V, Corkum P B and Villeneuve D M 2010 *Nature* **466** 604
51. Goulielmakis E, Loh Z-H, Wirth A, Santra R, Rohringer N, Yakovlev V S, Zherebtsov S, Pfeifer T, Azzeer A M, Kling M F, Leone S R and Krausz F 2010 *Nature* **466** 739
52. Ben-Nun M, Martínez T J, Weber P M and Wilson K R 1996 *Chem. Phys. Lett*. **262** 405
53. Niikura H, Villeneuve D M and Corkum P B 2005 *Phys. Rev. Lett*. **94** 083003
54. Chelkowski S, Yudin G L and Bandrauk A D 2006 *J. Phys. B* **39** S409
55. Debnarova A, Techert S, and Schmatz S 2006 *J. Chem. Phys*. **125** 224101
56. Schweigert I V and Mukamel S 2007 *Phys. Rev. A* **76** 012504
57. Mukamel S, Abramavicius D, Yang L, Zhuang W, Schweigert I V and Voronine D V 2009 *Acc. Chem. Res*. **42** 553
58. Smirnova O, Mairesse Y, Patchkovskii S, Dudovich N, Villeneuve D, Corkum P and Ivanov M Y 2009 *Nature* **460** 972
59. Baum P and Zewail A H 2009 *Chem. Phys*. **366** 2
60. Debnarova A, Techert S and Schmatz S 2010 *J. Chem. Phys*. **133** 124309
61. Krausz F and Ivanov M 2009 *Rev. Mod. Phys*. **81** 163
62. Werner H-J, Knowles P J, Manby F R, Schütz M, Celani P, Knizia G, Korona T, Lindh R, Mitrushenkov A, Rauhut G, Adler T B, Amos R D, Bernhardsson A, Berning A, Cooper D L, Deegan M J O, Dobbyn A J, Eckert F, Goll E, Hampel C, Hesselmann A, Hetzer G, Hrenar T, Jansen G, Köppl C, Liu Y, Lloyd A W, Mata R A, May A J, McNicholas S J, Meyer W, Mura M E, Nicklass A, Palmieri P, Pflüger K, Pitzer R, Reiher M, Shiozaki T, Stoll H, Stone A J, Tarroni R, Thorsteinsson T, Wang M and Wolf A 2010 *Molpro, version 2010.1, a package of ab initio programs*, see http://www.molpro.net
63. Becke A. D 1993 *J. Chem. Phys*. **98** 5648
64. Lee C, Yang W and Parr R G 1998 *Phys. Rev. B* **37** 785
65. Dunning T H 1989 *J. Chem. Phys*. **90** 1007
66. Stapelfeldt H and Seideman T 2003 *Rev. Mod. Phys*. **75** 543
67. Leibscher M, Averbukh I S and Rabitz H 2003 *Phys. Rev. Lett*. **90** 213001
68. Leibscher M, Averbukh I S and Rabitz H 2004 *Phys. Rev. A*. **69** 013402
69. Seideman T and Hamilton E 2006 *Adv. At. Mol. Opt. Phys*. **52** 289
70. Worth G A, Beck M H, Jäckle A and Meyer H-D 2007 The MCTDH Package, Version 8.2, (2000). H-D Meyer, Version 8.3 (2002), Version 8.4. See http://mctdh.uni-hd.de
71. Wang L, Meyer H-D and May V 2006 *J. Chem. Phys*. **125** 014102
72. Schröder M, Carreón-Macedo J L, and Brown A 2008 *Phys. Chem. Chem. Phys*. **10** 850
73. Combes J M, Grossmann A and Tchamitchian P 1989 *Wavelets* (Springer-Verlag, Berlin)
74. Chandre C, Wiggins S and Uzer T 2003 *Physica D* **181** 171
75. Milošević D B, Paulus G G, Bauer D and Becker W 2006 *J. Phys. B.: At. Mol. Opt. Phys*. **39** R203
76. Bandrauk A D, Chelkowski S and Shon N. H 2002 *Phys. Rev. Lett*. **89** 283903

77. Hartke B, Kosloff R and Ruhman S 1989 *Chem. Phys. Lett*. **158** 238
78. Banin U, Bartana A, Ruhman S and Kosloff R 1994 *J. Chem. Phys*. **101** 8461
79. Sathyamurthy N 1992 *Lasers in chemical and biological sciences* (Wiley Eastern, New Delhi) pp. 19–29
80. Kühn O and Wöste L (eds) *Analysis and control of ultrafast photoinduced reactions*, (Springer-Verlag Berlin)
81. Ruhman S and Kosloff R 1990 *J. Opt. Soc. Am. B* **7**, 1748
82. Cerullo G, Bardeen C J, Wang Q and Shank C V 1996 *Chem. Phys. Lett*. **262** 1362
83. Mishima K and Yamashita K 1999 *J. Chem. Phys*. **110** 7756
84. Sathyamurthy N and Joseph T 1984 *J. Chem. Edu*. **61** 968
85. Belz S, Grohmann T and Leibscher M 2009 *J. Chem. Phys*. **131** 034305
86. Deeb O, Leibscher M, Manz J, von Muellern W and Seideman T 2007 *ChemPhysChem* **8** 322
87. Nagashima K and Takatsuka K 2009 *J. Phys. Chem. A* **113** 15240
88. Yonehara T and Takatsuka K 2009 *Chem. Phys*. **366** 115
89. Okuyama M and Takatsuka K 2009 *Chem. Phys. Lett*. **476** 109